Metastable rhombohedral Fe phase formed in Fe/Sb multilayers and its magnetic properties

F. Pan, M. Zhang, M. Ding, and B. X. Liu
Department of Materials Science and Engineering, Tsinghua University, Beijing 100084, China

Y. M. Zhou and D. S. Wang
Laboratory for Surface Physics, Institute of Physics and Center for Condensed Matter Physics, Chinese Academy of Science, Beijing 100080, China

(Received 11 June 1998; revised manuscript received 21 September 1998)

Fe/Sb multilayer films with various Fe and Sb layer thicknesses were prepared by vapor deposition. A metastable rhombohedral Fe phase was formed in the Fe/Sb multilayered films, when the Fe layer thickness was of 1.7 nm and the Sb layer thickness was of 10 nm. In an opposite condition, a metastable bcc Sb phase was obtained, when the Fe layer was thicker than 4 nm and the Sb layer was thinner than 2.5 nm. Interestingly, the metastable rhombohedral Fe exhibited ferromagnetic behavior and its average magnetic moment was as high as $1.52\mu_B$. The magnetic behavior and electronic and magnetic structures of the rhombohedral Fe were calculated by the first-principles all-electron linearized augmented plane-wave method (LAPW) within the local spin-density functional approximation. The difference between the calculation of the Fe magnetic-moment amplitude ($3.32\mu_B$) and the experimental determination ($1.52\mu_B$) was discussed in terms of the presence of dead layers at the Fe/Sb interfaces. [S0163-1829(99)02017-2]

I. INTRODUCTION

In the last decade, magnetic multilayered films on a nanometer scale with artificial periodicity have attracted much attention because these films may feature some anomalous magnetic properties, such as changes in magnetization as the magnetic layer thickness is reduced, appearance in some cases of a uniaxial interfacial anisotropy, and giant magnetoresistance. These phenomena are probably correlated with the role of surface and interface states as dimensions become lower, e.g., the reduced coordination number and symmetry of atoms, formation of metastable phase, interface roughness accompanied by chemical disordering, etc.[1–4] In Fe-metal multilayers, some metastable Fe phases were obtained in some systems by various deposition methods, and these films behaved with different magnetic behavior. For example, Himpsel[5] and Macedo, Keune, and Ellerbrock[6] reported that fcc Fe grew epitaxially on Cu single crystals. In our recent study,[3] Fe grew also in fcc structure on polycrystalline Cu by electron-beam vapor deposition. In Fe/Pt, Fe/Pd, and Fe/Ti systems, fcc Fe was also observed by Croft *et al.*[7] and Zhang, Pan, and Liu[8,9] and it exhibited ferromagnetic behavior.[10] The hcp metastable Fe was formed in Fe/Ru superlattices with short periodicity by Maurer *et al.*[11] Besides, amorphous Fe was observed in Fe/Zr and Fe/Dy multilayers.[12–14] The observation of these metastable iron phases provides a way to explore the origin of the magnetization of the magnetic materials. With extensive data obtained for many multilayers systems, several models have been proposed for predicting the magnetization of the films.[1–2,15–20] The models generally rely on electron-spin density of the iron atom in an ideal magnetic-nonmagnetic interface or in the transitional structure sublayer (interface mixing). For example, based on an all-electron total-energy local spin-density approach, Freeman and co-workers[15–16] predicted that there would be a significant enhancement in two-dimensional magnetism at surfaces and interfaces in transition metals grown on noble metals. Tight-binding calculations of the magnetic surface, interface, and multilayers by Krompiewski and others[2,17] gave a similar prediction. Kübler's calculation revealed that both fcc and hcp bulk Fe phases should undergo a transition to a magnetic state at volume expansions of the order of 5%.[21–22] An alternative explanation for the magnetic modification in some Fe/metal films may be attributed to the so-called interface ''dead layer'' [11,18–19] or ''active layer'' proposed by some researchers.[20] However, there is no good model to explain completely all the experimental results obtained in the Fe/metal films so far. Hence it is of interest to study further the magnetization of various metastable phases formed in Fe/metal films. The purpose of this paper is to get a metastable Fe phase to investigate the magnetic properties of this metastable phase. In Fe/Sb system, the atomic configurations in the (001) plane of rhombohedral Sb and in the (111) plane of bcc Fe are quite similar, and the atomic distances in the (001) Sb and (111) Fe were of 0.4307 and 0.4053 nm, respectively, i.e., a difference in their atomic distance is only 5.9%. It is possible to form a rhombohedral metastable Fe phase from a crystallographic point of view. Fe/Sb multilayers were therefore selected to get a rhombohedral metastable Fe phase. In this paper, we report a rhombohedral metastable Fe phase observed in the Fe/Sb multilayers prepared by electron-beam vapor deposition and its magnetic properties, the correlation between the magnetic properties and the microstructure emerged in the films, and we discuss the possible mechanisms responsible for the observations. Besides, the magnetic behaviors and electronic and magnetic structures of the rhombohedral Fe were also investigated by the first-principles all-electron linearized augmented plane-wave method (LAPW) in the local spin-density functional approximation.

II. EXPERIMENTAL PROCEDURE

The Fe/Sb multilayered films were prepared by depositing alternatively pure iron (99.99%) and antimony (99.9999%) at rates of 0.05–0.2 nm/s onto NaCl single-crystal chips with a freshly cleaved surface (for microstructure studies) and glass substrates 0.1 mm thick (for magnetic property measurement) in an electron-beam evaporation system at a vacuum level of 1×10^{-4} Pa. The first layer on the substrate was antimony. The thickness of the constituent metals (t_{Fe} and t_{Sb}) varied from 1–10 nm which was controlled by a quartz monitor in the evaporation system. The total thickness of the films was approximately 40 nm (for microstructure studies) and 120 nm (for magnetic property measurement), respectively. Samples were analyzed by transmission electron microscopy (TEM), selected area diffraction (SAD), and x-ray diffraction to identify the crystalline structure. Rutherford-backscattering spectroscopy (RBS) was employed to measure the thickness, periodicity, and chemical composition of the samples. The magnetic properties were measured with a vibrating-sample magnetometer (VSM), with a resolution of 5×10^{-6} emu, in a magnetic field of up to 10 kOe at room temperature. The size of the VSM samples was 4×6 mm. First, a hysteresis loop of the substrate together with the holder was measured and the saturation magnetization M_s was found to be about 1×10^{-4} emu, which was one to two orders of magnitude lower than that of the studied Fe/metal multilayered films. Then the hysteresis loops of the samples were measured and the magnetization of the substrate and holder were subtracted automatically by the computer. To reduce the experimental error, measurements were made on an assembly of five similar specimens. Consequently, the magnetic moment from the substrate and holder had a negligible effect on the measured values, and the precision of the measured magnetic moment of the films was estimated to be better than 1%. After measuring the magnetic properties, the films were dissolved in a 5 ml HNO_3 and the inductively coupled plasma atomic emission spectrum (ICP) was employed to determine the Fe content in the multilayered films. An average magnetic moment per Fe atom was then obtained using above data. The error involved in the ICP measurement was about 5% and the total error for the magnetic moment was therefore around 6%.

III. RESULTS AND DISCUSSION

A. Microstructure of the Fe/Sb multilayers

1. Determination of the periodicity

Low angle x-ray-diffraction and RBS results indicated that the composition, thickness, and periodicity of all the samples agreed with the nominal values. For instance, Fig. 1 shows a typical low angle x-ray-diffraction pattern of the $[\mathrm{Fe}(4.0\,\mathrm{nm})/\mathrm{Sb}(3.7\,\mathrm{nm})]_{20}$ (the subscript is the number of the Fe/Sb bilayers) multilayers. From this pattern, the third- and fourth-order diffraction peaks of the Fe/Sb multilayer can clearly be seen at 3.42 and 4.62°, respectively, which give a modulation periodicity of the multilayers to be 7.7 nm. Figure 2 shows a RBS spectrum of $[\mathrm{Fe}(4.0\,\mathrm{nm})/\mathrm{Sb}(10.0\,\mathrm{nm})]_{10}$ multilayers. The spectrum was obtained with 2.023 MeV He^+ ions and the laboratory backscattering angle was 165°. From the spectrum, one can see two peaks. The high channel

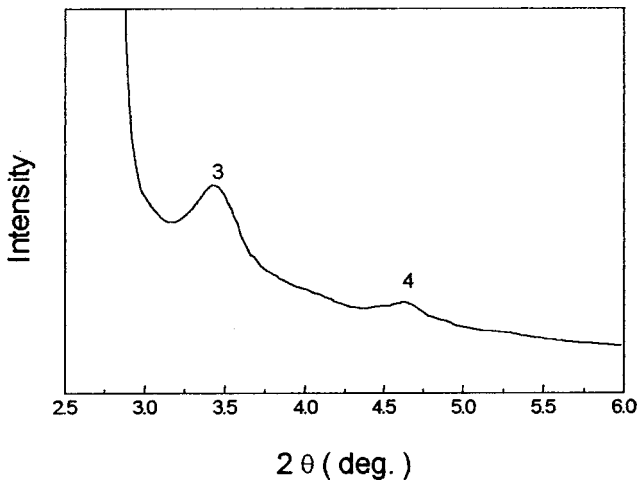

FIG. 1. The typical low angle x-ray-diffraction pattern of the $[\mathrm{Fe}(4.0\,\mathrm{nm})/\mathrm{Sb}(3.7\,\mathrm{nm})]_{20}$ multilayers.

one is from the Sb and the low channel is from the Fe. Although the detector used at these energies has insufficient energy resolution (about 10 nm) to resolve the individual layers, the Sb peak at its low-energy edge and the highest channel of the Fe signal can still be distinguished. By calculating the area and width of the Fe and Sb peaks, the total thickness is estimated to be about 140 nm, and the average thickness of each Fe and Sb layers agrees with the nominal deposited thickness. The same Fe/Sb periodicity of the Fe/Sb multilayers was also confirmed by the ICP measurement. In short, the characterization results confirmed that all the samples had a periodic structure along the normal to the films.

2. Microstructure analysis

The microstructure of the films was investigated by TEM SAD analysis. The experimental results revealed that the structure of Fe/Sb multilayers varied strongly with the variation of the layer thickness of the constituent metals. Figure 3 shows the SAD patterns of Fe/Sb multilayers with various Fe thicknesses, while the Sb layer thickness was kept at 10 nm. From Fig. 3(a), one can see that, when $t_{Fe}\leqslant1.7$ nm and $t_{Sb}=10$ nm, there is only one rhombohedral phase in the films,

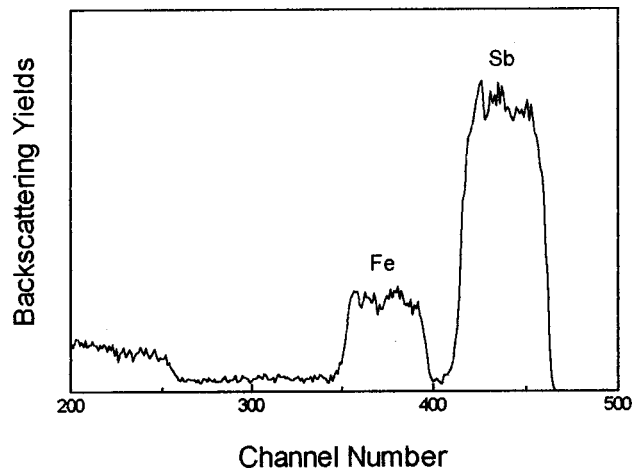

FIG. 2. The RBS spectrum of $[\mathrm{Fe}(4.0\,\mathrm{nm})/\mathrm{Sb}(10.0\,\mathrm{nm})]_{10}$ multilayers.

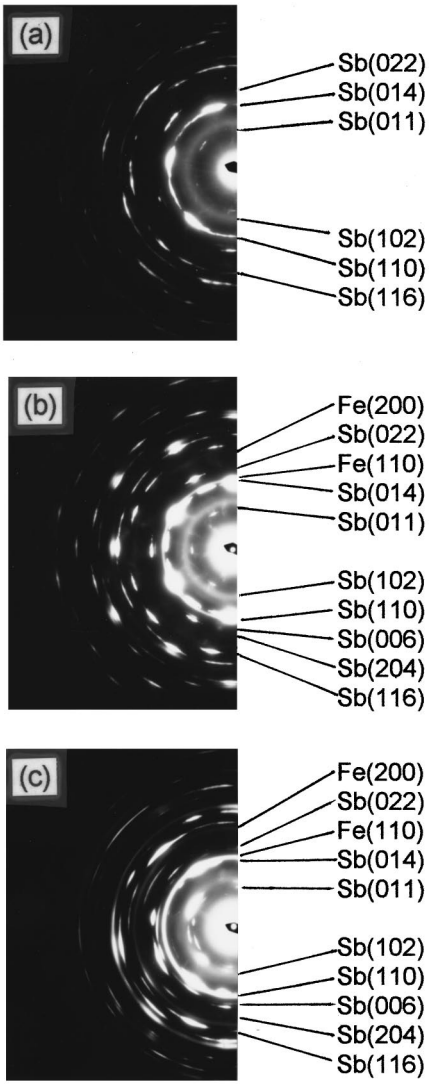

FIG. 3. The typical TEM SAD pattern of the Fe/Sb multilayers with various Fe thicknesses, while the Sb layer thickness was kept at 10 nm: (a) Fe(1.7 nm)/Sb(10.0 nm); (b) Fe(2.5 nm)/Sb(10 nm); (c) Fe(4.0 nm)/Sb(10.0 nm).

and its lattice parameters are determined to be $a=0.450\pm0.005$ nm and $\alpha=57.1°$ (i.e., $a=0.431\pm0.005$ nm and $c=1.127\pm0.005$ nm for hexagonal lattice), which are exactly the same of those of the pure Sb. When t_{Fe} reaches 2.5 nm, in addition to the diffraction lines from the rhombohedral phase, a bcc Fe (110) diffraction line emerges as shown in Fig. 3(b), indicating that the bcc Fe phase is formed in the films, i.e., the films consists of bcc Fe and rhombohedral Sb. From Fig. 3 it can also be found that when $t_{Sb}=10$ nm, the Sb grain size of the Fe/Sb films decreased with increasing t_{Fe}, which results in the diffraction lines in the SAD pattern having an increasing tendency from discontinuous to continuous. The average Sb grain size of the films was about 35, 20, and 2 μm when $t_{Fe}=1.7$, 2.5, and 4.0 nm, respectively, while the grain size of the bcc Fe was in a nanoscale, i.e., about 5–10 nm.

There are two possible mechanisms for the formation of only one rhombohedral phase in Fe/Sb multilayers, in which the Fe layers are thinner than 1.7 nm. First, the Fe atom might grow in a rhombohedral structure on polycrystalline rhombohedral Sb layers. Second, a rhombohedral solid solution might be formed at the Fe/Sb interfaces. According to the low angle x-ray-diffraction results, the films had a good periodic structure along the normal to the films. Besides, the lattice parameters of the observed rhombohedral phase is the same as that of pure Sb and the solubility of Fe in Sb is almost nil.[23] It could therefore be thought that, under our experimental conditions, the Fe atoms grew in a rhombohedral structure on thick Sb layer, which was similar to that some metastable Fe phases grew epitaxially in the Fe-base multilayers, e.g., a hcp Fe phase grew in Ru/Fe superlattice,[11] fcc Fe phases grew in Fe/Cu (Refs. 3 and 5) and Fe/Pt (Ref. 8) multilayers.

From a crystallographic point of view, the rhombohedral structure Fe phase formed on the thick Sb layer was also possible, because the atomic configurations in the (001) plane of rhombohedral Sb and in the (111) plane of bcc Fe are quite similar, and the atomic distances in the (001) Sb and (111) Fe were of 0.4307 and 0.4053 nm, respectively, i.e., a difference in their atomic distance is only 5.9%.

It should be noted that the structure discussed in this study was based on the analyses of results by TEM SAD, one can say that the experimental evidences of the rhombohedral structure Fe phase formed in the Fe/Sb multilayers are weak, because it is possible that the signal coming from the 1.7 nm Fe layer is too weak to be observable. Recalling our previous studies,[3,10] it can be found that, for Fe/Cu and Fe/Pd multilayers with the same total thickness of Fe/Sb ones, when the Fe layer thickness was 1.2 nm (lower than 1.7 nm), the diffraction lines from Fe phase can be clear observed by TEM SAD, i.e., if bcc Fe existed in the films, it would be detected by TEM SAD. These observations supported above argue that bcc Fe wasn't formed in the Fe/Sb multilayers, which provide an indirect evidence of the rhombohedral structure Fe phase formed in the Fe/Sb films. If the multilayers are characterized by extended x-ray-absorption fine structure or cross-section TEM investigations, detailed knowledge of the local structure could be obtained, this certainly deserves further study.

When t_{Fe} is thicker than 2.5 nm, the Fe atoms cannot grow in a rhombohedral structure because of the internal stress caused by a large mismatch between Fe and Sb, resulting in the formation of bcc Fe in the films. Figures 3(b) and 3(c) are the SAD patterns of Fe(2.5 nm)/Sb(10 nm) and Fe(4.0 nm)/Sb(10 nm) samples, respectively, showing the diffraction lines from the rhombohedral Sb and bcc Fe phases.

We also studied the possibility of growth of metastable bcc Sb on thick Fe layers in Fe/Sb multilayers. It turned out that when the Sb layer is thin and Fe layer is relatively thick, i.e., when $t_{Sb}=2.5$ nm and $t_{Fe}\geqslant4.0$ nm, there are only diffraction lines from a bcc phase appearing in the SAD patterns, and its lattice parameter is just the same of that of pure Fe (0.2866 nm). In other words, the metastable bcc Sb phase grew on thick Fe layer. For example, Fig. 4 is a SAD pattern of the Fe(8.0 nm)/Sb(2.5 nm) sample, showing only bcc diffraction lines. The grain size in the sample was about 10 nm, which is much smaller than that in the Fe/Sb films with $t_{Sb}=10.0$ nm.

Figure 5 shows the SAD patterns of the Fe/Sb multilayers with various Sb thicknesses, while the Fe layer thickness was

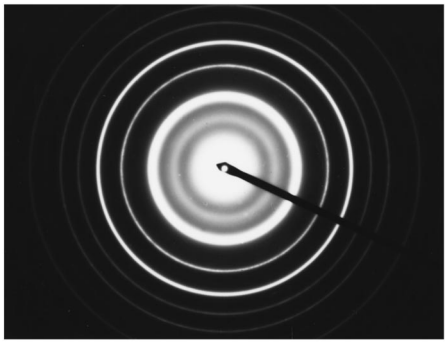

FIG. 4. The typical TEM SAD pattern of the Fe(8.0 nm)/Sb(2.5 nm) sample, showing only bcc diffraction lines.

kept at 2.5 nm. One can see that, though the films consisted of bcc Fe and the rhombohedral Sb phases, the Sb grain size of the samples increased obviously with increasing t_{Sb}, i.e., it was about 10 nm, 10 μm, and 20 μm for Fe(2.5 nm)/Sb(2.5 nm), Fe(2.5 nm)/Sb(6.0 nm), and Fe(2.5 nm)/Sb(10.0 nm) films, respectively, while the grain size of the bcc Fe was in a nanoscale, i.e., about 5–10 nm.

From Figs. 3, 4, and 5 it can also be found that, when $t_{Sb} > t_{Fe}$, the diffraction rings of the samples were discontinuous. These patterns indicated that texture structures were present in the films with some specific orientation relationships, yet the texture was not very distinct as diffraction rings still appeared. The textured decreased with increasing t_{Fe} and with decreasing t_{Sb}, respectively, and eventually the texture orientation disappeared. For example, there was no texture in the Fe(8.0 nm)/Sb(2.5 nm) films. The Sb grain size of the films can be changed from 50~10 nm for the Fe(8.0 nm)/Sb(2.5 nm) to 35 000 nm (i.e., 35 μm) for Fe(1.7 nm)/Sb(10.0 nm) films.

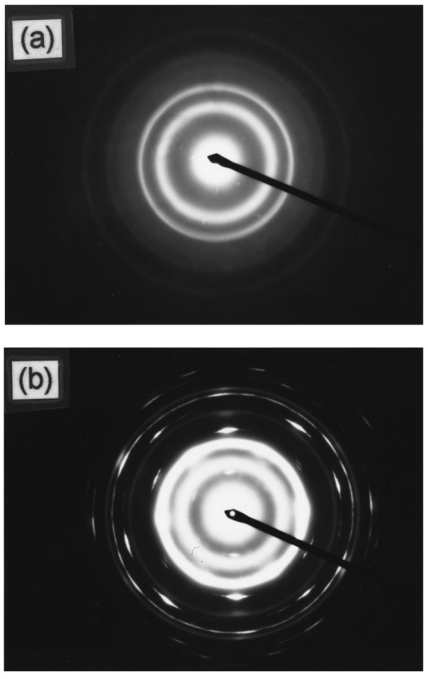

FIG. 5. The TEM SAD patterns of the Fe/Sb multilayers with various Sb thicknesses, while the Fe layer thickness was kept at 2.5 nm: (a) Fe(2.5 nm)/Sb(2.5 nm) and (b) Fe(2.5 nm)/Sb(6.0 nm).

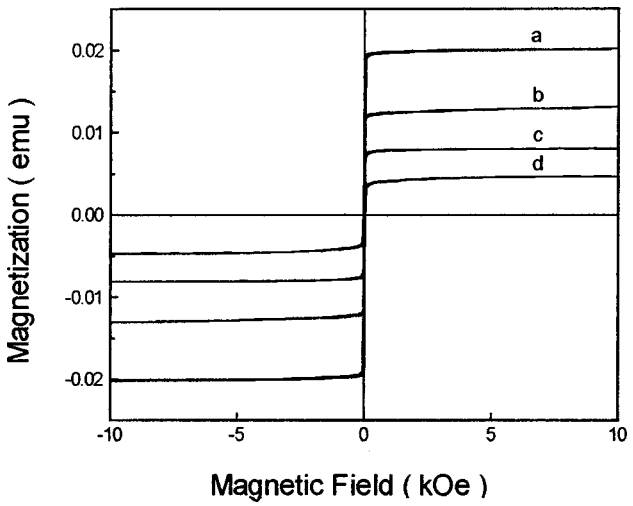

FIG. 6. The hysteresis loops of Fe/Sb multilayers in a magnetic field of up to 10 kOe parallel to the film plane: (a) Fe(6.0 nm)/Sb(2.5 nm); (b) Fe(4.0 nm)/Sb(2.5 nm); (c) Fe(4.0 nm)/Sb(6.0 nm); and (d) Fe(1.7 nm)/Sb(10.0 nm).

B. Magnetic properties of the films

To obtain a better understanding of the rhombohedral Fe phase formed in the Fe/Sb multilayers, the magnetic properties of the films were studied by VSM at room temperature. Figure 6 shows the hysteresis loops of the Fe/Sb multilayers in a magnetic field of up to 10 kOe parallel to the film plane. Table I shows the average magnetic moment per Fe atom in Fe/Sb multilayers. From Fig. 6 and Table I one can see that all the Fe/Sb multilayers, including the films with rhombohedral Fe, are ferromagnetic and have an in-plane easy axis of magnetization. The magnetic moment per Fe atom in Fe/Sb multilayers was about the same as in the bulk Fe when $t_{Fe} = 8.0$ nm and $t_{Sb} = 2.5$ nm, and it decreased with decreasing t_{Fe}. For Fe(1.7 nm)/Sb(10.0 nm) multilayers, the magnetic moment per Fe in the rhombohedral structure can still be as high as $1.52\mu_B$. In the previous works it was found that some solid solution (or amorphous phase) could be formed in the Fe/metal interface, and the solid solution exhibited paramagnetic behavior at room temperature.[12–14,24] Recalling the microstructural results of the films (Fig. 3), if the solid solution was formed in the Fe(1.7 nm)/Sb(10.0 nm) films, the sample would have very low magnetization. In our case, Fe(1.7 nm)/Sb(10.0 nm) films had higher magnetization, which suggested that the Fe layer did not grow in solid solution. In other words, the magnetic measurement provided

TABLE I. The average magnetic moment per Fe atom (μ_B) in Fe/Sb multilayers for various t_{Fe} and t_{Sb}.

		Thickness of Fe layer (t_{Fe} nm)				
		1.7	2.5	4.0	6.0	8.0
	1.4		1.658			
Thickness of Sb layer (t_{Sb} nm)	2.5		1.728	1.796	1.651	2.190
	3.7		1.704			
	6.0		1.683			
	10.0	1.520	1.806	1.767		

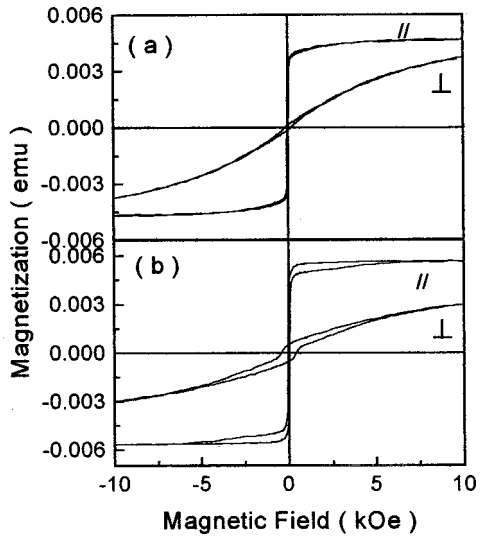

FIG. 7. The hysteresis loops of the Fe/Sb multilayers measured with the magnetic field parallel and perpendicular to the film plane for (a) Fe(1.7 nm)/Sb(10.0 nm) and (b) Fe(4.0 nm)/Sb(10.0 nm).

an indirect evidence for the formation of a metastable Fe phase in a rhombohedral structure and the new phase can behave ferromagnetically with a high magnetic moment.

Figure 7 shows two hysteresis loops of the Fe/Sb multilayers measured with the magnetic field parallel and perpendicular to the film plane. From the figure, the saturation field, for the perpendicular case, depended on the thickness of the Fe layer when $t_{Sb}=10$ nm. Saturating the Fe(1.7 nm)/Sb(10.0 nm) multilayers was much easier than saturating the Fe(4.0 nm)/Sb(10.0 nm) ones. This revealed that as the t_{Fe} decreased, there was an increasing tendency for perpendicular magnetization in the Fe/Sb multilayers, which was similar to those observed in Fe/noble-metal multilayers.[3,10,25–26]

Concerning the effect of film structure on the magnetic properties of the Fe/Sb multilayers, as mentioned above, even though the grain size of Sb phase varied obviously with t_{Fe} and t_{Sb}, the grain size of bcc Fe was almost the same in all films, i.e., about 5–10 nm, which might mainly relate to the evaporation conditions of the samples, except the grain size of Fe phase was large in Fe(1.7 nm)/Sb(10 nm) multilayers owing to the epitaxial growth of the metastable rhombohedral Fe phase. Therefore, in our case, the grain size of films had a small effect on the magnetic properties of the films. From Table I, one can see that the magnetic moment of the Fe/Sb films varied with t_{Fe} and t_{Sb}, i.e., it decreased with decreasing t_{Fe}, which was probably related to the spin orientational configuration of the Fe atoms under the action of the Sb layer. According to the experimental results of a Mössbauer spectroscopy analysis by Maurer *et al.*,[11] a so-called interface ''dead layer'' existed in the multilayers, i.e., two interfacial layers bear no moment, similar results were also reported by Sato and others.[27–29] The relative thickness of dead layer (i.e., the thickness ratio of the nonmagnetic Fe layer to the magnetic Fe layer) increased with decreasing t_{Fe}, results in the above observed magnetic properties, i.e., the magnetic moment of the films with thin Fe layer was lower than that with thick Fe one.

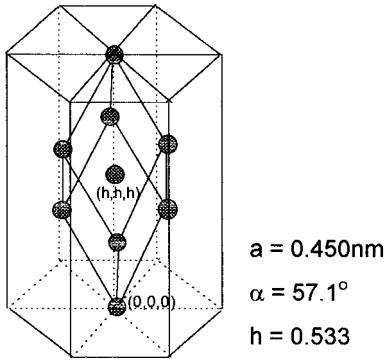

FIG. 8. The crystallographic lattice unit cell containing two atoms of the metastable rhombohedral Fe phase.

C. Simulation of the magnetic moment of the rhombohedral Fe phase

The rhombohedral Fe phase formed in Fe/Sb and its magnetic properties, to our knowledge, have not been reported previously. To interpret the observations and to probe the reason for the magnetic behaviors, the electronic and magnetic structure of the rhombohedral Fe was investigated by the first-principles all-electron linearized augmented plane-wave method (LAPW) (Refs. 19–21) in the local spin-density functional approximation. A crystallographic lattice unit cell which includes two atoms at (0, 0, 0) and (0.533, 0.533, 0.533) is used for convenience of programming (see Fig. 8). The lattice constant was selected from $a=0.405$ to 0.475 nm, while $\alpha=57.1°$. The basis size used in solving the eigenvalue problem was more than 50 LAPW's per atom and 4096 special k points in the first Brillouin zone of the rhombohedral unit cell were used to generate electron density. Core change density was computed self-consistently in a fully relativistic Dirac-Slater-type atomic structure program for every iteration and valence states are computed semirelativistically, i.e., the Dirac equation is solved including mass velocity and Darwin terms but without the spin-orbit coupling term. No shape approximations were made for the potential and charge density in the interstitial region, but the potential was assumed spherically symmetric inside the muffin-tin spheres.[19–21,30,31] The convergence measured by

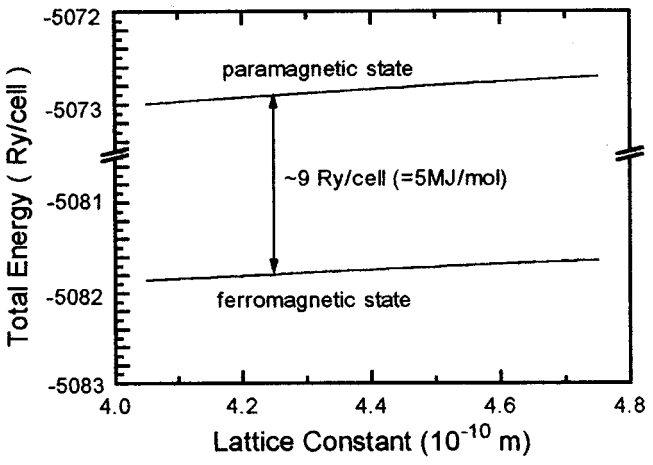

FIG. 9. The calculated total energy per atom of the rhombohedral Fe phase with various lattice constants.

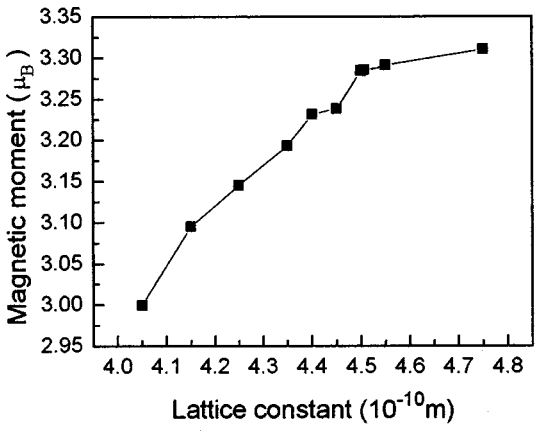

FIG. 10. The calculated magnetic moment per atom as a function of the lattice constant for the ferromagnetic (FM) state of the rhombohedral Fe phase.

the rms difference between input and output was better than 1 mRy for the sum of spin-up and spin-down potential (or 0.05 me/a.u.^{3} for charge density) and better than 0.02 mRy for their difference (or 0.005 me/a.u.^{3} for spin density).

Figure 9 shows the calculated total energy per atom of the rhombohedral Fe phase with various lattice constants. From this figure, one can see that all the calculated total energies of the ferromagnetic (FM) and the paramagnetic (PM) states increase with increasing lattice constant and that the calculated total energy of the FM state was about 9.0 Ry/cell ($\sim$5 MJ/mol) lower than that of PM state of rhombohedral Fe phase, suggesting the ground state of the rhombohedral Fe phase is the FM state.

Figure 10 gives the calculated magnetic moment per atom as a function of the lattice constant for the FM state of the rhombohedral Fe phase. The calculated magnetic moment per Fe atom in rhombohedral structure was about $3.23\mu_B$ when the lattice constant was 0.450 nm (i.e., $a=0.431$ nm and $c=1.127$ nm for hexagonal lattice) and it decreased with decreasing lattice constant of the rhombohedral Fe phase.

It is noted that there is a difference in magnetic moment between the calculated and experimentally measured values. This is also related to the so-called ''die layer.'' In calculation of the magnetic moment of the rhombohedral Fe phase, the spin orientational configuration of the Fe atoms under the action of the Sb layer hadn't been taken into simulation of the magnetic moment. According to the experimental results of a Mössbauer spectroscopy analysis by Maurer *et al.*,[11] in hexagonal Fe/Ru superlattices with short periodicity, the internal Fe layer carry a moment of about $2\mu_B$, whereas the two interfacial layers bear no moment, i.e., the interface ''dead layer'' existed in the multilayers. In our case, according to the mean magnetic moment per Fe atom and the structural parameter of the Fe(1.7 nm)/Sb(10.0 nm) multilayers, the effective Fe layer was calculated as $1.7\times1.52/3.23=0.8$ nm, in which 3.23 was the calculated magnetic moment of bulk rhombohedral Fe phase by the first-principles all-electron linearized augmented plane-wave method (LAPW) (Refs. 19–21) in the local spin-density functional approximation. Therefore the thickness of the nonmagnetic Fe layer per interface in Fe(1.7 nm)/Sb(10.0 nm) was $1.7\times(1-1.52/3.23)/2=0.45$ nm, i.e., about two to three Fe monolayers, which agreed with the value in Fe/Ru films.[11] Hence, the above calculation can serve as a support to our experimental observations as well as the above discussed interpretation in a qualitative way.

IV. CONCLUSION

In summary, we have shown experimental evidence of a metastable rhombohedral Fe phase obtained in the Fe/Sb multilayers with $d_{Fe}\leqslant1.7$ nm and $d_{Sb}\geqslant10$ nm. The rhombohedral Fe metastable phase exhibits ferromagnetic behavior and its average magnetic moment in the Fe(1.7 nm)/Sb(10.0 nm) multilayers is $1.52\mu_B$. The magnetic behavior and electronic and magnetic structures of the rhombohedral Fe were calculated by the first-principle all-electron linearized augmented plane-wave method (LAPW) in the local spin-density functional approximation. The difference between the calculation of the Fe magnetic moment amplitude ($3.23\mu_B$) and the experimental determination ($1.52\mu_B$) was thought to relate with the dead layers probably formed at the Fe/Sb interfaces.

ACKNOWLEDGMENT

This work was supported in part by the National Natural Science Foundation of China and by the Administration of Tsinghua University.

[1] A. J. Freemam and R. Wu, J. Magn. Magn. Mater. **104–107**, 1 (1992).
[2] S. Krompiewski, U. Krauss, and U. Krey, J. Magn. Magn. Mater. **92**, L295 (1991).
[3] B. X. Liu and F. Pan, Phys. Rev. B **48**, 10 276 (1993).
[4] S. S. P. Parkin, Appl. Phys. Lett. **58**, 1473 (1991).
[5] F. J. Himpsel, Phys. Rev. Lett. **67**, 2363 (1991).
[6] W. A. A. Macedo, W. Keune, and E. D. Ellerbrock, J. Magn. Magn. Mater. **93**, 552 (1991).
[7] M. Croft, D. Sills, A. Sahiner, A. F. Jankowski, P. H. Ansari, E. Kemly, F. Lu, Y. Jeon, and T. Tsakalakos, Nanostruct. Mater. **9**, 1 (1997).
[8] M. Zhang, F. Pan, and B. X. Liu, J. Phys.: Condens. Matter **9**, 7623 (1997).
[9] M. Zhang, F. Pan, and B. X. Liu, J. Magn. Magn. Mater. **182**, 89 (1998).
[10] F. Pan, T. Yang, J. Zhang, and B. X. Liu, J. Phys.: Condens. Matter **5**, L507 (1993).
[11] M. Maurer, M. Piecuch, M. F. Raver, J. C. Ousset, J. P. Sánchez, C. Aaron, J. Dekoster, D. Raoux, A. De Andres, M. De Santis, A. Fontaine, F. Baudelet, J. L. Rouvière, and B. Dieny, J. Magn. Magn. Mater. **93**, 15 (1991).
[12] J. Landes, Ch. Sauer, B. Kabius, and W. Zinn, Phys. Rev. B **44**, 8342 (1991).
[13] S. Kraegermann, F. Stobiecki, T. Stobiecki, and K. Roell, J. Magn. Magn. Mater. **101**, 209 (1991).
[14] J. Dubowik, F. Stobiecki, H. Rohrmann, and K. Roll, J. Magn. Magn. Mater. **152**, 201 (1996).

[15] A. J. Freeman and C. L. Fu, J. Appl. Phys. **61**, 3356 (1987).
[16] C. L. Fu, A. J. Freeman, and T. Oguchi, Phys. Rev. Lett. **54**, 2700 (1985).
[17] J. Tersoff and L. M. Falicov, Phys. Rev. B **26**, 6186 (1982).
[18] C. S. Wang and A. J. Freeman, J. Magn. Magn. Mater. **15/18**, 869 (1980).
[19] R. H. Victora and L. M. Falicov, Phys. Rev. B **28**, 5232 (1983).
[20] R. Krishnan and M. Tessier, J. Appl. Phys. **67**, 5391 (1990).
[21] V. L. Moruzzi, P. M. Marcus, and J. Kübler, Phys. Rev. B **39**, 6957 (1989).
[22] J. Kübler, Solid State Commun. **72**, 631 (1989).
[23] Colin James Smithells, *Smithells Metals Reference Book*, 6th ed., edited by Eric A. Brandes (Butterworth, London, 1983), pp. 11–256.
[24] K. Yoden, N. Hosoito, K. Kawaguchi, K. Mibu, and T. Shinjo, Jpn. J. Appl. Phys., Part 1 **27**, 1680 (1988).
[25] H. J. G. Draaisma, W. J. M. de Jonger, and F. J. A. den Broeder, J. Magn. Magn. Mater. **66**, 351 (1987).
[26] C. J. Gutierrez, S. H. Mayer, and J. C. Walker, J. Magn. Magn. Mater. **80**, 299 (1989).
[27] N. Sato, J. Appl. Phys. **61**, 1979 (1987).
[28] F. Pan, Y. D. Fan, K. Tao, and B. X. Liu, Phys. Status Solidi A **153**, 481 (1996).
[29] D. D. Koelling and G. O. Arbman, J. Phys. F **5**, 2041 (1975).
[30] H. Krakauer, M. Posternak, and A. J. Freeman, Phys. Rev. B **19**, 1706 (1979).
[31] M. Posternak, H. Krakauer, A. J. Freeman, and D. D. Koelling, Phys. Rev. B **21**, 5601 (1980).